

The Leptophilic Dark Matter in the Sun: the Minimum Testable Mass

Zheng-Liang Liang,^{1,*} Yi-Lei Tang,^{2,†} and Zi-Qing Yang^{3,‡}

¹*Institute of Applied Physics and Computational Mathematics
Beijing, 100088, China*

²*School of Physics, KIAS,
85 Hoegiro, Seoul 02455, Republic of Korea*

³*Big Data Research, IFLYTEK
Wangjiang Road West 666#, Hefei, 230088, China*

Abstract

The physics of the solar dark matter (DM) that are captured and thermalise through the DM-nucleon interaction has been extensively studied. In this work, we consider the leptophilic DM scenario where the DM particles interact exclusively with the electrons through the axial-vector coupling. We investigate relevant phenomenologies in the Sun, including its capture, evaporation and thermalisation, and we calculate the equilibrium distribution using the Monte Carlo methods, rather than adopting a semi-analytic approximation. Based on the analysis, we then determine the minimum testable mass for which the DM-electron coupling strength can be probed via the neutrino observation. Compared to the case of the DM-nucleon interaction, it turns out that minimum detectable mass of the DM-electron interaction is roughly 1 GeV smaller, and a cross section about two orders of magnitude larger is required for the saturation of the annihilation signal.

*Electronic address: liangzl@itp.ac.cn

†Electronic address: tangyilei@kias.re.kr

‡Electronic address: ziqingyang@google.com

1. INTRODUCTION

Several neutrino telescopes have been looking for the trace of the Weakly Interacting Massive Particles (WIMPs) [1–4], a generic kind of candidate for the Dark Matter (DM), from the Sun. This is based on the picture that the Galactic WIMPs collides with nuclei in the Sun as they pass by the solar neighbourhood, gradually sinking into the solar core after subsequent collisions, and end up annihilating into primary or secondary neutrinos that escape the environment of the dense plasma in the Sun, so to be observed by the terrestrial neutrino detectors.

The neutrino flux at the detector location is related to the solar DM annihilation through the following schematic relation:

$$\frac{d\Phi_\nu}{dE_\nu} = \frac{\Gamma_A}{4\pi d_\odot^2} \frac{dN_\nu}{dE_\nu}, \quad (1.1)$$

where d_\odot is the Sun-Earth distance, $d\Phi_\nu/dE_\nu$ and dN_ν/dE_ν represent the neutrino differential flux at the Earth and the neutrino energy spectrum per DM annihilation event in the Sun, respectively. The total annihilation rate Γ_A can be expressed in terms of the number of the trapped DM particles N_χ :

$$\Gamma_A = \frac{1}{2} A_\odot N_\chi^2, \quad (1.2)$$

where A_\odot denotes twice the annihilation rate of a pair of DM particles. The evolution of the solar DM number N_χ is depicted with the following equation:

$$\frac{dN_\chi}{dt} = C_\odot - E_\odot N_\chi - A_\odot N_\chi^2, \quad (1.3)$$

which involves the DM capture (evaporation) rate C_\odot (E_\odot) by scattering off atomic nuclei in the Sun, as well as the annihilation rate A_\odot . Eq. (1.3) has an analytic solution

$$N_\chi(t) = \frac{C_\odot \tanh(t/\tau_e)}{\tau_e^{-1} + (E_\odot/2) \tanh(t/\tau_e)}, \quad (1.4)$$

with

$$\tau_e = (C_\odot A_\odot + E_\odot^2/4)^{-1/2} \quad (1.5)$$

the time scale for the capture, evaporation and annihilation processes to equilibrate. Once the equilibrium is reached at the present day, *i.e.*, $\tanh(t_\odot/\tau_e) \simeq 1$, with $t_\odot = 4.5 \times 10^9$ yr being the solar age, the annihilation output Γ_A also reaches its maximum value. Depending on the ratio $E_\odot^2/(C_\odot A_\odot)$, or the DM mass m_χ , such equilibrium can be categorized into two different scenarios: (1) $E_\odot^2/(C_\odot A_\odot) \ll 1$, that's when the evaporation effect can be neglected and the equilibrium is between annihilation and capture. In this case, $N_\chi \simeq C_\odot/E_\odot$ and hence $\Gamma_A \simeq C_\odot/2$, so we can either determine or constrain the strength of the DM-nucleon interaction from solar neutrino observation; (2) $E_\odot^2/(C_\odot A_\odot) \gg 1$, under this circumstance evaporation overwhelms annihilation for the DM depletion, and the balance

between evaporation and capture yields $N_\chi \simeq \sqrt{C_\odot/A_\odot}$ and $\Gamma_A \simeq A_\odot C_\odot^2 / (2 E_\odot^2)$, which not only implies a heavy suppression of the neutrino flux, but also prevents us from drawing the coupling strength of the DM-nucleon interaction from the possible observed signals.

While relevant phenomenology associated with the DM-nucleon interaction have been studied extensively in literature, the tempting possibility that the DM particles couple exclusively to leptons, the so-called leptophilic scenario, has aroused wide interest in the community [5–13]. However, even for a broad range of leptophilic DM models, it turns out that the effective DM-nucleon cross section arising from the loop-induced DM-quark interaction competes with or overwhelms that of the DM-electron interaction [7]. A notable exception is that the DM particle interacts with electron through the axial-vector coupling, a case in which the loop-induced contribution vanishes.

In this work, we will investigate some interesting phenomena of the leptophilic DM trapped in the Sun. Specifically, we will explore the minimum testable mass through neutrino observation for the scenario where the DM particle couples exclusively to electron. The minimum detectable solar DM mass is determined by the parametric relations between capture, evaporation and annihilation, as has been extensively studied in the context of the DM-nucleon coupling scenario [14–34]. But considering that the medium of the ionised electrons is much softer than that of the nuclei (suppressed by a factor $\sqrt{m_e/m_N}$ in terms of thermally averaged momentum, with the electron (nucleus) mass m_e (m_N)), the minimum detectable leptophilic DM mass is expected to be smaller accordingly, due to the less energetic collisions that would prevent the buildup of the solar DM through evaporation. While quantitative analyses on this issue have been discussed in ref. [31], where equilibrium distribution of leptophilic DM was described phenomenologically with a semi-analytic approximation, in this paper, we will pursue an accurate evaluation of the distribution with a Monte Carlo method adopted in refs. [17, 29, 35], in an effort to provide a more precise description of the leptophilic DM in the Sun. Interestingly, we find that the simulated distribution is remarkably suppressed at the high velocity end when compared to the truncated Boltzmann approximation adopted in ref. [31], and results in an evaporation rate roughly 4 orders of magnitude smaller. As a consequence, such difference translates to an evaporation mass around 1 GeV smaller.

This paper is organised as follows. In sec. 2, we will take a brief review on the theoretical ground for the capture, evaporation, and annihilation of the leptophilic DM in the Sun, and put these formulas into numerical computation. Main results, along with relevant analyses and discussions, are provided in sec. 3.

2. DISTRIBUTION AND EVOLUTION OF SOLAR DM

In this section we will discuss the distribution and evolution of the solar DM. An accurate description of the distribution of the captured DM is crucial for the evaluation of evaporation and annihilation rate, and together with capture rate, they determine the evolution of the solar DM population. We obtain the solar DM distribution by solving the Boltzmann equation in a numerical manner. Now we delve into the details.

2.1. capture of the dark matter by solar electrons

The buildup of the solar DM population begins with the capture of the Galactic DM particles. There is the possibility that the free-streaming DM particles will be gravitationally pulled inside the Sun and scattered by electrons therein to velocities lower than the local escape velocity, so to be captured. The standard procedure for evaluating the DM capture rate \widetilde{C}_\odot has been well established in the literature [19, 36, 37]. After a small modification to replace nuclei with electrons, the capture rate of the DM particle by solar electrons can be expressed as

$$\widetilde{C}_\odot = \frac{\rho_\chi}{m_\chi} \int_0^{R_\odot} 4\pi r^2 dr \int \frac{w}{u} g_\chi(\mathbf{u}) d^3u \int_0^{v_{\text{esc}}} R_e(w \rightarrow v) dv, \quad (2.1)$$

where R_\odot is the radius of the Sun, m_χ is the mass of the DM particle, ρ_χ and $g_\chi(\mathbf{u})$ are the DM density in the solar neighborhood and the velocity distribution in the solar rest frame, respectively. In calculation, we use $\rho_\chi = 0.3 \text{ GeV} \cdot \text{cm}^{-3}$ and model the velocity distribution as a Maxwellian form in the rest frame of the Galactic centre, with the dispersion velocity $v_0 = 220 \text{ km} \cdot \text{s}^{-1}$ and a truncation at the Galactic escape velocity of $544 \text{ km} \cdot \text{s}^{-1}$. $w = \sqrt{v_{\text{esc}}^2 + u^2}$ connects the velocity outside the solar influence sphere, u , and the one accelerated by the gravitational pull at the radius r , with the local escape velocity v_{esc} . The quantity $R_e^-(w \rightarrow v)$ represents the differential event rate of a DM particle with initial velocity w down-scattered to final smaller one v by solar electrons in unit volume as the following,

$$\begin{aligned} R_e^-(w \rightarrow v) &= n_e \left\langle \frac{d\sigma_{\chi e}}{dv} |\mathbf{w} - \mathbf{u}_e| \right\rangle \\ &= n_e \int f_e(\mathbf{u}_e) \frac{d\sigma_{\chi e}}{dv} |\mathbf{w} - \mathbf{u}_e| d^3u_e, \end{aligned} \quad (2.2)$$

where the differential cross section for the DM-electron system $d\sigma_{\chi e}/dv$ depends on their relative velocity $\mathbf{w} - \mathbf{u}_e$, and $\langle \dots \rangle$ denotes the average over the thermal velocity distribution of solar electrons. n_e is the local electron number density. The Maxwellian distribution $f_e(\mathbf{u}_e)$ is written as

$$f_e(\mathbf{u}_e) = (\sqrt{\pi} u_0)^{-3} \exp\left(-\frac{u_e^2}{u_0^2}\right), \quad (2.3)$$

with $u_0 = \sqrt{2 T_\odot / m_e}$. $T_\odot(r)$ is the local temperature at radius r . Hence the event rate eq. (2.2) can be further expressed explicitly in the following analytic form,

$$\begin{aligned} R_e^-(w \rightarrow v) &= \frac{n_e \sigma_{\chi e}}{4\eta} (\eta^+)^2 \frac{v}{w} \left\{ \text{erf} \left[\frac{(\eta^- w - \eta^+ v)}{2u_0}, \frac{(\eta^- w + \eta^+ v)}{2u_0} \right] \right. \\ &\quad \left. + \exp[\eta(w^2 - v^2)/u_0^2] \text{erf} \left[\frac{(\eta^+ w - \eta^- v)}{2u_0}, \frac{(\eta^+ w + \eta^- v)}{2u_0} \right] \right\}, \end{aligned} \quad (2.4)$$

where $\eta^\pm \equiv \eta \pm 1 = m_\chi/m_e + 1$, and $\text{erf}(a, b) \equiv \text{erf}(b) - \text{erf}(a)$.

2.2. relaxation and distribution of the solar DM

In order to determine the distribution of the trapped DM, in this work we adopt the numerical method outlined in ref. [17], which is in essence equivalent to solving the Boltzmann equation. The benefits are two-fold: first, this method is able to describe the high end of the velocity distribution of the solar DM, which is a prerequisite of an accurate evaluation of evaporation rate; second, this method can also provide a detailed description of the relaxation process of the newly captured DM particles. The second advantage is especially important because in contrast to the nucleus capture scenario, the marginally captured DM particles by solar electrons are prone to be ejected back to deep space before their distribution reach the final equilibrium. The leakage due to the evaporation over the relaxation process needs to be carefully quantified.

Here we take a brief introduction to the methodology. Our discussion is based on the assumption that the accumulated DM population does *not* bring any significant impact on the solar structure, *i.e.*, the Sun as a heat reservoir is also modeled as the background for the residing DM particles. We keep track of a small portion of DM particles since their capture until they finally integrate into the rest already in equilibrium. The Boltzmann equation is linear due to the absence of the DM self-interaction*, and can be further simplified as the following *master equation* if expressed with a convenient choice of parameters E (total energy per mass) and L (angular momentum per mass) [17]:

$$\begin{aligned} \frac{df(E, L, t)}{dt} &= -f(E, L, t) \sum_{E', L'} S(E, L; E', L') + \sum_{E', L'} f(E', L', t) S(E', L'; E, L) \\ f(E, L, 0) &= f_{\text{cap}}(E, L), \end{aligned} \quad (2.5)$$

where $f(E, L, t)$ is distribution function at time t , and $S(E, L; E', L')$ represents the scattering matrix element for transition process $(E, L) \rightarrow (E', L')$. In practice the parameters E and L are nondimensionalised in terms of an energy reference value GM_{\odot}/R_{\odot} , and an angular momentum value $(GM_{\odot}R_{\odot})^{1/2}$. These values are constructed from a length unit, namely the solar radius $R_{\odot} = 6.955 \times 10^5$ km, and a time unit $(GM_{\odot}/R_{\odot}^3)^{-1/2} = 1.596 \times 10^3$ s, with the Newton's constant G and the solar mass $M_{\odot} = 1.988 \times 10^{30}$ kg.

As mentioned in ref. [29], in the optical thin limit and for a large enough time step Δt , the probability for a collision in simulation is insensitive to the starting position in the periodic orbit defined by E and L , so these two parameters are sufficient for the representation of DM states bound to the Sun. The initial distribution $f_{\text{cap}}(E, L)$ is obtained by assuming the DM particles captured after first collision with electrons do not deviate much from their incident directions. Consequently, if ϑ is defined as the angle between the trajectory of scattered DM particle and radial direction from the centre of the Sun, the probability distribution scale proportionally with differential $d(\cos \vartheta)$ in each spherical layer $4\pi r^2 dr$, with $0 \leq \vartheta \leq \frac{\pi}{2}$. For illustration, we present the initial distribution $f_{\text{cap}}(E, L)$ for a 2 GeV DM particle in the

* Since only a small increment of solar DM particles is under investigation, annihilation effects can be all attributed to solar DM particles already in equilibrium. A detailed discussion is arranged at the end of sec. 3

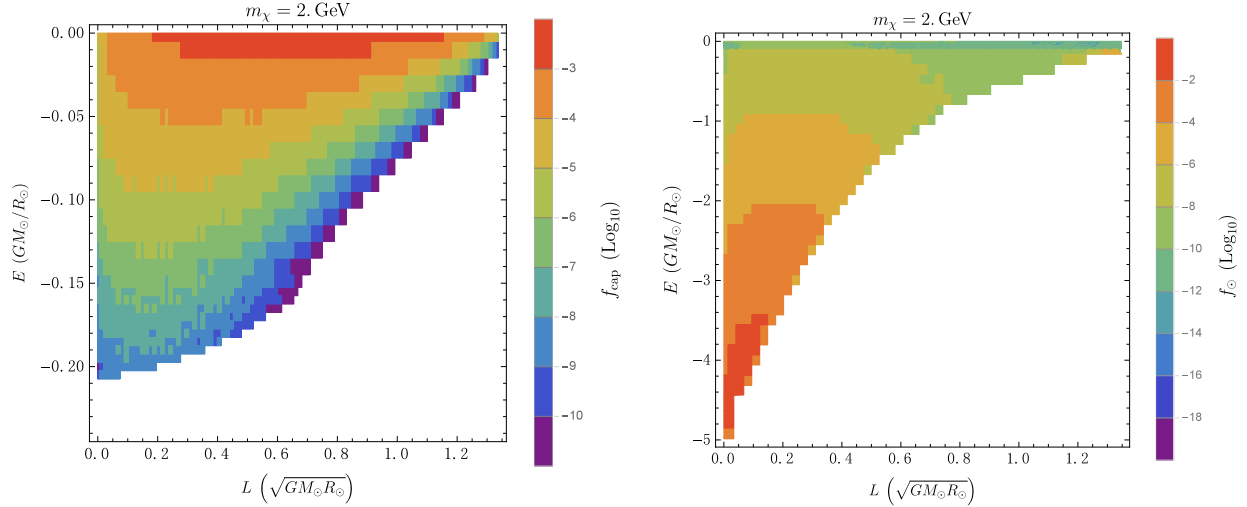


Figure 2.1: Initial distribution $f_{\text{cap}}(E, L)$ (left) and the limit distribution f_\odot (right) of a 2 GeV DM particle, respectively. The energy E and angular momentum L are nondimensionalised in units of GM_\odot/R_\odot and $(GM_\odot R_\odot)^{1/2}$, respectively. Only the coloured parameter region is allowed for bound orbits in the *right* panel. See text for details.

left panel of fig. 2.1.

It should be noted that compared with nucleus, the electron thermal momentum is suppressed by $\sqrt{m_e/m_N}$, which suggests that the DM particle can only marginally fall into, and easily escape from the solar gravitational well. Therefore the evaporation effect is taken into account in eq. (2.5), at variance with the approach adopted in ref. [29], where only gravitationally bound states are involved in the simulation of relaxation process. This modification is necessary considering that the leakage due to evaporation may no longer be neglected over the relaxation process. Since all bound states are connected and the evaporated DM particles are not anticipated to be trapped again, in simulation we allocate one state to account for the escape state that is corresponding to the *absorbing* state in the context of Markov process, whereas all bound states are corresponding to the *transient* states. For long enough time, evaporation will deplete all the DM particles participating in simulation, but before that a steady normalised distribution among the survival DM particles is expected to be reached (for which we provide a proof in Appendix A). We evolve eq. (2.5) with the discrete time step Δt until $f(E, L)$ converges to this limiting distribution $f_\odot(E, L)$, and other physical details of the relaxation can be recorded at the same time. The equilibrium distribution $f_\odot(E, L)$ is shown in the right panel of fig. 2.1.

In practice, we use different levels of resolution to represent the bound states on the E - L plane. In order to accurately describe the transitions that occur mostly near the escape state, the absolute value of energy (angular momentum) parameter E (L) is logarithmically (uniformly) discretised in 40 (500) states from 0.01 (0) to 0.1 (1.35), and all bound states with energy above -0.01 are represented by $E = -0.01$, which is equivalent to imposing a cutoff above 0.995 of the escape velocity on the distribution. The second and the third regions are uniformly divided into 35×50 pieces on the E - L plane from 0.1 (0) to 4.5 (1.35),

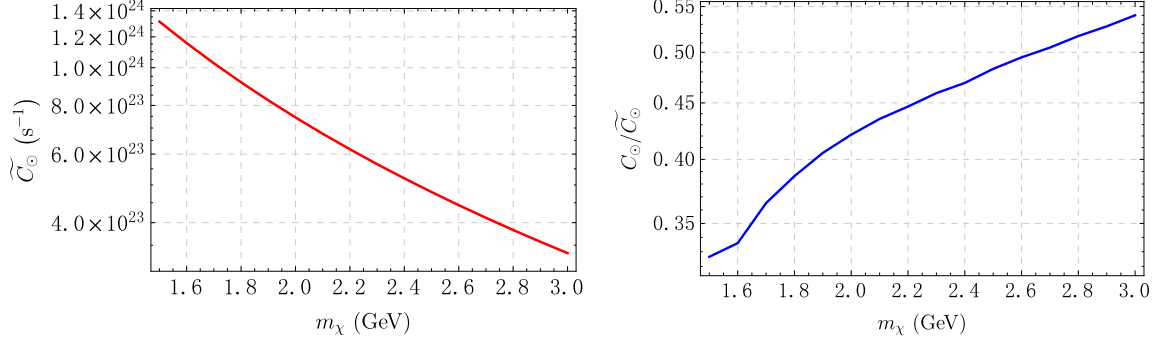


Figure 2.2: (*left*) The original capture rate for the DM mass range from 1.5 to 3.0 GeV, obtained from eq. (2.1). (*right*) Relevant ratio of the effective capture rate to the original one, $C_\odot/\widetilde{C}_\odot$. See text for details.

and 10×20 pieces from 4.5 (0) to 5.04 (1.35), respectively. If the relaxation time scale is verified to be much smaller than the Sun age t_\odot (or τ_e), the picture of instant thermalisation will keep unchanged except that an effective capture rate C_\odot should be introduced as the original one \widetilde{C}_\odot , suppressed by the remaining proportion over the relaxation process. For illustration, the capture rate \widetilde{C}_\odot and the ratio between the two capture rates, $C_\odot/\widetilde{C}_\odot$, are presented in fig. 2.2, respectively.

The scattering matrix element $S(E, L; E', L')$ is determined with Monte Carlo approach. Specifically, a large number of DM random walk samples are generated and tallied in the fixed time step Δt , which is required to be long enough to ensure that the test particle receive substantial transfer momentum from solar electrons. The periodic radial trajectory of the bound DM particle between successive collisions is numerically integrated with the Standard Sun Model (SSM) GS98 [38] inside the Sun ($r \leq 1$), and is matched to analytic Keplerian orbit beyond the solar radius (if any). Thus the $(i+1)$ -th collision location and time t_{i+1} can be determined with the random renewal collision probability P_c^i via

$$P_c^i = 1 - \exp \left[- \int_{t_i}^{t_{i+1}} \lambda(\tau) d\tau \right], \quad (2.6)$$

where

$$\begin{aligned} \lambda &= n_e \langle \sigma_{\chi e} (|\mathbf{w} - \mathbf{u}_e|) |\mathbf{w} - \mathbf{u}_e| \rangle \\ &= n_e \sigma_{\chi e} \left[\frac{u_0}{\sqrt{\pi}} \exp(-w^2/u_0^2) + \left(w + \frac{u_0^2}{2w} \right) \operatorname{erf} \left(\frac{w}{u_0} \right) \right] \end{aligned} \quad (2.7)$$

is *implicitly* dependent on the temporal parameter τ once the DM trajectory is determined with the method mentioned above. By generating further random numbers that help pick out the colliding solar electron's velocity, and the scattering angle in the centre-of-mass (CM) frame, we then determine the outgoing state of the scattered DM particle after a coordinate transformation back to the solar reference.

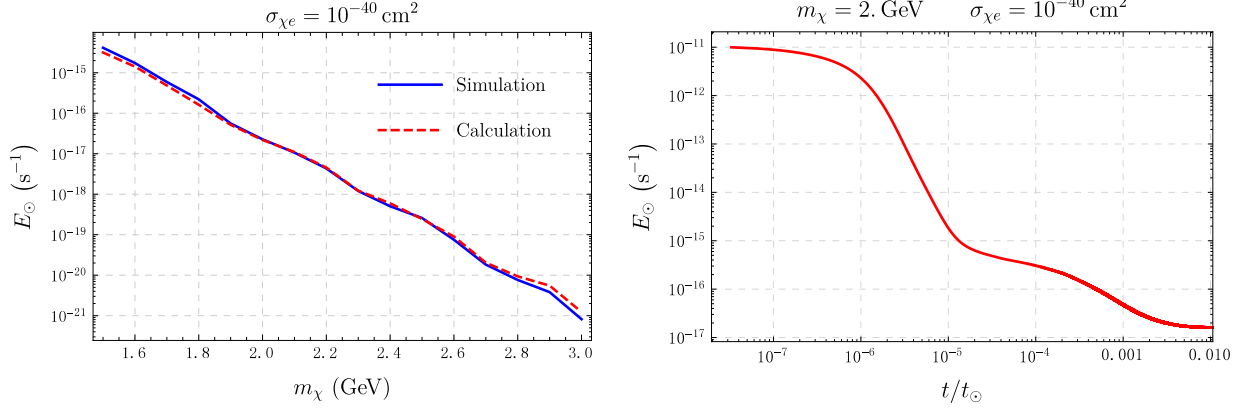


Figure 2.3: *Left*: Evaporation rate of the equilibrium state for the DM mass range from 1.5 to 3.0 GeV, obtained from simulation and calculation, respectively. *Right*: Evolution of the evaporation rate for a 2 GeV DM from its initial captured state to the equilibrium state, against a time scale of the solar age t_\odot . See text for details.

2.3. evaporation and annihilation

Given the distribution, both evaporation and annihilation rate of the bound DM particle can be determined. The theoretical expression of the evaporation rate differs with the capture rate only in the way that the distribution of the incident DM particles is replaced by the normalised distribution of the DM particles trapped in the Sun, $f_\odot(r, w)$, and an up-scatter event rate $R_e^+(w \rightarrow v)$ with $v > w$ is introduced to account for the evaporation rather than $R_e^-(w \rightarrow v)$. Thus the evaporation rate is expressed as

$$E_\odot = \int_0^{R_\odot} dr \int f_\odot(r, w) dw \int_{v_{\text{esc}}}^{+\infty} R_e^+(w \rightarrow v) dv, \quad (2.8)$$

where

$$R_e^+(w \rightarrow v) = \frac{n_e \sigma_{\chi e}}{4\eta} (\eta^+)^2 \frac{v}{w} \left\{ \text{erf} \left[\frac{(\eta^+ v - \eta^- w)}{2u_0}, \frac{(\eta^+ v + \eta^- w)}{2u_0} \right] + \exp[\eta(w^2 - v^2)/u_0^2] \text{erf} \left[\frac{(\eta^- v - \eta^+ w)}{2u_0}, \frac{(\eta^- v + \eta^+ w)}{2u_0} \right] \right\}. \quad (2.9)$$

Besides, the evaporation rate can also be determined from simulation straightforwardly. Specifically speaking, the evaporation rate can also be constructed by collecting all the inflow probability into the escape state in each time step, at any instant time during the evolution of solar DM. Evaporation rates obtained from these two approaches are found quite consistent in our study. For illustration in the left panel of fig. 2.3 shown are the relevant evaporation rates for a benchmark cross section $\sigma_{\chi e} = 10^{-40} \text{ cm}^2$ and the DM mass ranging from 1.5 to 3.0 GeV, with the blue solid line representing the evaporation rate drawn from the simulation, and the red dashed line corresponding to the calculated one. In the right panel of fig. 2.3, we present the simulated evolution of the evaporation rate for a 2 GeV DM. The time scale is expressed in terms of the solar age t_\odot . From the right panel

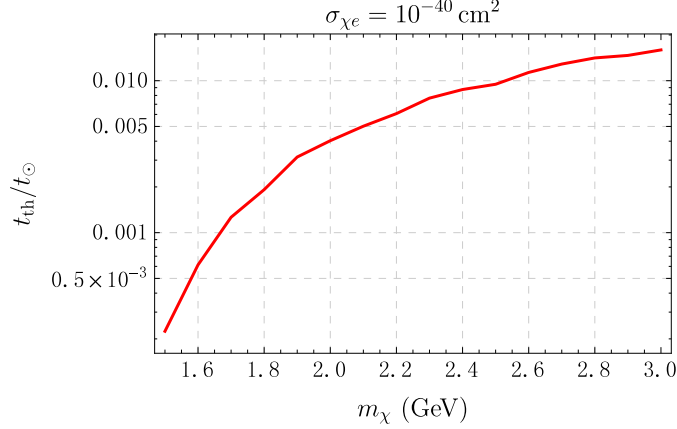


Figure 2.4: The thermalisation time of the captured solar DM particles in the simulation.

of fig. 2.3, the thermalisation time t_{th} can also be determined once the evaporation rate is observed to reach its convergence. For illustration, we present the simulated thermalisation time for cross section $\sigma_{\chi e} = 10^{-40} \text{ cm}^2$ in fig. 2.4.

It is interesting to compare above evaporation rate with the one given in ref. [31], where a Maxwell-Boltzmann form is assumed for the solar DM distribution. By requiring that the net heat transfer between the DM particles and the solar elements equal zero, the effective temperature T_χ of the DM isothermal distribution and hence the evaporation rate can be determined. In fig. 2.5 we present the comparison between the two velocity distributions of a 2 GeV DM particle. In the left panel, the simulated velocity distribution f_χ is shown in the blue, while the approximated Maxwell-Boltzmann form f_χ^{MB} is shown in the red, with an effective temperature $T_\chi \approx 0.845 T_\odot$ (0) drawn from ref. [31]. While the bulks of two velocity distributions truncated at the escape velocity are found to be basically consistent, it turns out that the simulated ones fall off much more rapidly at the high velocity end where evaporation substantially occurs, which consequently results in greatly suppressed evaporation rates. As shown in the right panel, the ratio between the two distributions, $f_\chi/f_\chi^{\text{MB}}$, is significantly suppressed especially at the high velocity tail, leading to an evaporation rate around 4 orders of magnitude smaller. Such suppression has also been observed in the case of DM-nucleon interaction in comparison between the two approaches [16, 17, 29], but the extent is much slighter because in such case only a finite part of evaporation events take place around the local escape velocity where the suppression is remarkable. Considering that the evaporation rate is highly sensitive to tail of the velocity distribution, we perform three simulations to generate sufficient statistics to examine the robustness of our results. Owing to the fine grids representative of the high-energy bound states on the E - L plane, these simulated distributions at the high velocity end are found to be quite consistent, and evaporation error is confined within 15%, corresponding to a variation in evaporation mass of 0.013 GeV [†].

[†] Conventionally, one used the evaporation mass m_{evp} defined through the equation $E_\odot(m_{\text{evp}}) = t_\odot^{-1}$ as a rough estimate of the DM masses above which the evaporation effects can be neglected. It is straightforward to read from the slope in fig. 2.3 that a variation of 15% of evaporation rate translates to a displacement of the evaporation mass around 0.013 GeV.

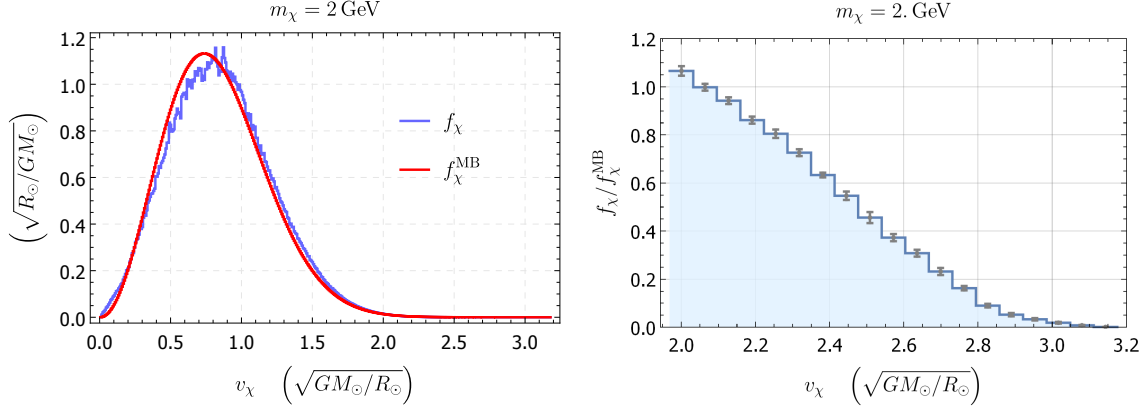


Figure 2.5: *Left*: velocity distributions of 2 GeV DM particle obtained from simulation (blue) and Maxwell-Boltzmann approximation truncated at escape velocity with an effective temperature $T_\chi \approx 0.845 T_\odot$ (0) (red), respectively. The two distributions extend to no further than the escape velocity at the solar core $v_{\text{esc}}(0) \approx 3.17$. *Right*: the ratio between the simulated and the isothermal velocity distributions at the high velocity tail. See text for details.

Thus we omit the statistical errors originating from the simulation in our discussion.

On the other hand, the annihilation coefficient A_\odot is expressed in terms of the thermal cross section $\langle\sigma v\rangle_\odot$ and the effective occupied volume of the solar DM, V_{eff} , as the following:

$$A_\odot \equiv \frac{\langle\sigma v\rangle_\odot}{V_{\text{eff}}}, \quad (2.10)$$

if an s -wave thermal annihilation cross section is assumed. The effective volume is defined as

$$V_{\text{eff}} \equiv \frac{\left(\int_0^{R_\odot} n_\chi(r) 4\pi r^2 dr\right)^2}{\int_0^{R_\odot} n_\chi^2(r) 4\pi r^2 dr}, \quad (2.11)$$

with $n_\chi(r)$ being the number density of the solar DM, which in practice is also determined from simulation. Therefore, the effective volume can be approximated from the simulated equilibrium distribution as the following function:

$$V_{\text{eff}} = 5.67 \times 10^{29} \left(\frac{5 \text{ GeV}}{m_\chi}\right)^{2.15} \text{ cm}^3. \quad (2.12)$$

3. MINIMUM TESTABLE MASS OF THE LEPTOPHILIC DM

Based on the above numerical efforts on the capture, evaporation and annihilation of the leptophilic DM in the Sun, now we are ready to explore the parameter space where the solar neutrino observational approach is effective for the detection.

In analysis, we adopt the criterion $t_\odot/\tau_e \gtrsim 3.0$ or equivalently $\tanh(t_\odot/\tau_e) \simeq 1$ for the assumption that the neutrino flux reaches its full strength. On the other hand, in order

to specify the parameter region for the annihilation- and evaporation-dominated scenarios, we set the criteria as $E_\odot^2/(4A_\odot C_\odot) \leq 0.1$ and $E_\odot^2/(4A_\odot C_\odot) \geq 10$, respectively, where the canonical s -wave thermal annihilation cross section $\langle\sigma v\rangle_\odot = 3 \times 10^{-26} \text{ cm}^3 \cdot \text{s}^{-1}$ is adopted in definition (see eq. (2.10)).

The relevant parameter regions are presented in fig. 3.1. The quantitative analysis enables us to draw clear boundaries among different signal topologies. For instance, for a DM-electron cross section $\sigma_{\chi e} = 10^{-40} \text{ cm}^2$, the assumption of the equilibrium between capture and annihilation is only valid for a DM particle heavier than 1.94 GeV, while for a DM mass smaller than 1.72 GeV, one can no longer extract the coupling strength of the DM-electron interaction from the observed neutrino flux, because the number of DM particles $N_\chi \simeq C_\odot/E_\odot$ turns independent of cross section $\sigma_{\chi e}$. Moreover, if the cross section $\sigma_{\chi e}$ is smaller roughly than 10^{-41} cm^2 , the equilibrium among capture, evaporation and annihilation has not yet been reached at the present day. As a consequence, the signal flux is suppressed and the unsaturated number of the solar DM particles needs to be specified to determine or constrain the coupling strength [39]. For reference, in fig. 3.1 we also plot in yellow solid line the evaporation mass from the definition adopted in refs. [21, 31], where the minimum testable mass is defined as the one for which the number of captured DM particles differ with C_\odot/E_\odot at the 10% level

$$\left| N_\chi - \frac{C_\odot}{E_\odot} \right| = 0.1 N_\chi, \quad (3.1)$$

with N_χ defined in eq. (1.4). It is evident that our definition of the evaporation mass is a little stricter than the above one.

In above investigation on the parameter space for the leptophilic DM detection, the cross section is capped at $\sigma_{\chi e} = 10^{-36} \text{ cm}^2$, which corresponds to a mean free path $\ell_\chi(0) = (n_e(0)\sigma_{\chi e})^{-1} \approx 18 R_\odot$ at the centre of the Sun. As coupling strength increases, collisions between DM particles and electrons begin to be frequent in processes such as capture, evaporation and energy transfer, and hence the optically thin approximation will no longer be valid for the description of the solar DM. Due to the multiple collisions, evaporation will be suppressed and the minimum testable DM mass begin to decrease accordingly [31]. In that regime, the Monte Carlo approach adopted in this study will break down, since short DM free path requires an extra parameter for the description of the solar DM distribution, as mentioned in Sec. 2.2.2, and a full consideration of the Boltzmann equation is required, which is beyond the scope of this work.

Now we make some final remarks on the methodology adopted in this work, namely, to what extent is our calculation reliable considering that the DM depletion due to annihilation is not included in simulation of the relaxation process. To address this concern, we stress that it is the increment rather than the deposit of solar DM particles that we are simulating, and under this circumstance the annihilation effects can be all accounted for by the DM particles that have already settled in the Sun. To verify this, we first make a comparison between the differential annihilation rate and the effective capture rate with respect to the relaxation time scale t_{th} . During the time interval t_{th} , a number of $\Delta N_\chi \approx C_\odot t_{\text{th}}$ DM particles are trapped and participate in annihilation within the Sun, with the effective capture rate C_\odot

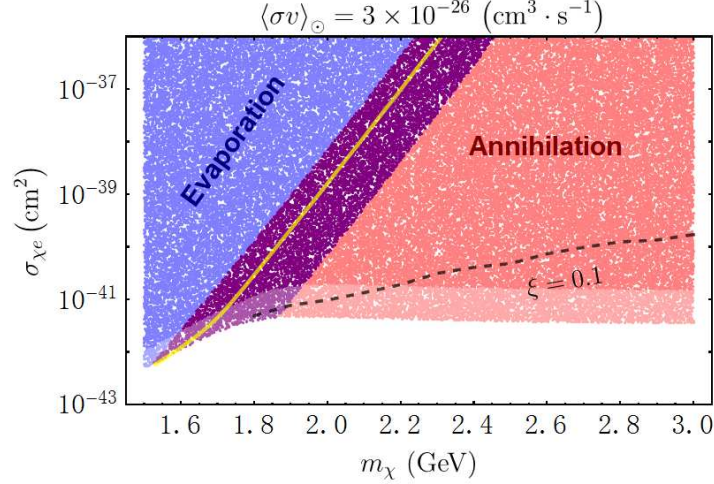


Figure 3.1: The parameter regions dependent on DM mass m_χ and the DM-electron cross section $\sigma_{\chi e}$. While the signal regions $\tanh(t_\odot/\tau_e) \simeq 1$ are presented as the coloured areas, the lighter parts correspond to the region where $0.9 \leq \tanh(t_\odot/\tau_e) \lesssim 1$ for reference. In the red (blue) area, annihilation (evaporation) plays the dominant role in the number evolution of the solar DM, and the purple belt represents the transition zone between the two extreme scenarios. The yellow solid line represents the evaporation mass defined in eq. (3.1). The black dashed line marks the contour of the parameter $\xi = 0.1$. See text for details.

involving the evaporation effect. ΔN_χ contributes approximately an annihilation rate of $2A_\odot(t) N_\chi(t) \Delta N_\chi$, where $N_\chi(t)$ is the number of the accumulated DM particles and $A_\odot(t)$ is the annihilation coefficient for corresponding equilibrium distribution at time t . It is noted that in contrast to the relaxation time scale t_{th} , here t should be regarded as a macroscopic temporal parameter. This is no other than the instant thermalisation assumption, and its validity will be scrutinised on a self-consistent basis in the following. The actual annihilation rate is expected to be smaller and hence more favourable to our reasoning because the initially captured DM particles reside mostly in high orbits, where annihilation events are much more rare than the case of equilibrium state. The accumulation of the solar DM particles continues until the gains and losses reach a balance, so one has $A_\odot(t) N_\chi(t) \Delta N_\chi \lesssim A_\odot N_\chi^2 (\Delta N_\chi/N_\chi) \lesssim C_\odot (\Delta N_\chi/N_\chi)$, with N_χ being the saturate number of the solar DM particles and corresponding annihilation coefficient A_\odot . The only assumption introduced here is that the *equilibrium* distribution at t approximately equals the one corresponding to the saturated number N_χ , so one has $A_\odot(t) \simeq A_\odot$. Its validity also relies on the instant thermalisation that will be investigated later. Above inequities indicates that, at the time scale of relaxation t_{th} , the annihilation rate due to the freshly captured DM particles can be well contained by the effective capture rate C_\odot . Especially, if condition $\Delta N_\chi/N_\chi \ll 1$ is satisfied, the differential annihilation rate can be neglected compared to the effective capture rate. In this case, the equation (now at a microscopic time scale) governing the evolution of the DM particles captured during time interval t_{th} regresses to a linear one, and the states of these DM particles at a microscopic time τ within $(0, t_{\text{th}})$ can be expressed as a linear superposition of states of independent samples captured during an arbitrary time interval

$\delta t (\ll t_{\text{th}})$, at different moments in the time sequence $\{0, \delta t, 2\delta t, \dots, \tau - \delta t, \min(\tau, t_{\text{th}})\}$. To be specific, the equation to describe the DM number can be written as

$$\frac{dN_{\chi}}{d\tau} = \widetilde{C}_{\odot} - E_{\odot}(\tau) N_{\chi}(\tau), \quad (3.2)$$

where the capture rate \widetilde{C}_{\odot} does not include the evaporation effects. By linearity, one can re-express Eq. (3.2) as

$$\frac{d(N_{\chi 0} + N_{\chi 1} + \dots N_{\chi n})}{d\tau} = \widetilde{C}_{\odot} - (E_{\odot 0}(\tau) N_{\chi 0}(\tau) + \dots E_{\odot n}(\tau) N_{\chi n}(\tau)), \quad (3.3)$$

or equivalently,

$$\begin{aligned} \frac{dN_{\chi, i}}{d\tau} &= -E_{\odot, i}(\tau) N_{\chi, i}(\tau) \\ \frac{dN_{\chi, 0}}{d\tau} &= \widetilde{C}_{\odot} - E_{\odot 0}(\tau) N_{\chi 0}(\tau), \end{aligned} \quad (3.4)$$

with $1 \leq i \leq n = \lfloor (\tau/\delta t) \rfloor$, where the evaporation rate $E_{\odot, i}(\tau)$ only depends on the i -th DM particle sample. In the optical thin regime, one can always take a small enough time interval δt for which the post capture collisions are too soon to occur, so the supply of freshly captured DM particles dominates the evolution of the 0-th sample, and Eq. (3.4) can be simplified as

$$\frac{dN_{\chi, 0}}{d\tau} = \widetilde{C}_{\odot}. \quad (3.5)$$

Once the DM number of the 0-th sample reaches the fixed value $N_{\chi, 0} = \widetilde{C}_{\odot} \cdot \delta t$, we change its label to $n+1$, and use the following equation to describe its state thereafter,

$$\frac{dN_{\chi, n+1}}{d\tau} = -E_{\odot, n+1}(\tau) N_{\chi, n+1}(\tau), \quad (3.6)$$

where the evaporation rate $E_{\odot, n+1}(\tau)$ does not depend on other samples of DM particles. Then we allocate one more sample labeled 0 to account for the capture effects and repeat above procedures.

Therefore, so far as the simulated DM increment is concerned, while the evaporation effect of the volatile DM particles is taken into full account, the annihilation effect can be reasonably neglected as long as the condition $\Delta N_{\chi}/N_{\chi} = C_{\odot} t_{\text{th}}/N_{\chi} \simeq \xi \equiv C_{\odot} t_{\text{th}} / \left[\sqrt{C_{\odot}/A_{\odot} + E_{\odot}^2/(4A_{\odot}^2)} - E_{\odot}/(2A_{\odot}) \right] \ll 1$ is fulfilled, where the saturate number is approximated as the analytic expression $N_{\chi} = C_{\odot} / (\sqrt{C_{\odot}A_{\odot} + E_{\odot}^2/4} + E_{\odot}/2)$ in eq. (1.4). From an effective perspective the relaxation process can be conceived as a buffer, and only those settle into the equilibrium state are considered as captured and subject to the ensuing annihilation.

Since the annihilation effect is not included in the DM effective capture rate C_{\odot} , N_{χ}/C_{\odot} is smaller than actual saturation time of the increasing solar DM number. In addition, considering that the annihilation grows to its maximum at N_{χ} and the relation $\xi \geq A_{\odot} N_{\chi}^2 t_{\text{th}}/N_{\chi}$, ξ

also imposes a cap on the strength of the perturbation to the distribution due to annihilation. So the criterion $\xi \ll 1$ also applies to the relaxation in response to the annihilation for the accumulated DM particles and lives up to a sufficient condition for the instant thermalisation. The instant thermalisation in turn validate the a priori assumption that $A_{\odot}(t) \simeq A_{\odot}$. As a self-consistency check, the contour lines of the ratio $\xi = 0.1$ is given in fig. 3.1 for the reference purpose. The parameter region above these contours corresponds to smaller ξ . While in the evaporation-dominated regime the annihilation effects can be safely ignored and evolution of solar DM particles can be well described by eq. (3.4), the instant thermalisation proves to be a reasonable assumption for most of the parameter region in the annihilation-dominated area. This justifies our treatment in which the DM particles are captured at an effective rate that includes only evaporation effects during the instant relaxation process, and participate in subsequent annihilation with the equilibrium distribution obtained from simulating the relaxation process.

Acknowledgments

YLT is supported by National Research Foundation of Korea (NRF) Research Grant NRF- 2015R1A2A1A05001869, and the Korea Research Fellowship Program through the National Research Foundation of Korea (NRF) funded by the Ministry of Science and ICT (2017H1D3A1A01014127).

Appendix A: relative probability distribution of the transient states

In this appendix we will prove that for the given amount of the captured DM particles, while suffer loss from evaporation, their relative probabilities will eventually evolve to a steady distribution. Towards this end, we consider a Markov process with finite discrete states, which is governed by the equation

$$\frac{dp_i(t)}{dt} = \sum_j \mathbb{W}_{ij} p_j(t), \quad (\text{A.1})$$

or in a compact form

$$\frac{dp(t)}{dt} = \mathbb{W} p(t), \quad (\text{A.2})$$

where \mathbb{W} is the transition matrix that describes the gains and losses between the $(n+1)$ -state probabilities p_i ($i = 0, 1, \dots, n$). Based on the following two properties of \mathbb{W} :

$$\begin{aligned} \mathbb{W}_{ij} &\geq 0, \quad \text{for } i \neq j; \\ \sum_i \mathbb{W}_{ij} &= 0, \quad \text{for each } j, \end{aligned} \quad (\text{A.3})$$

it is well known that regardless of the initial distribution $p(0)$, the probabilities of the $n+1$ states have a steady distribution in the long-time limit [40]. On the other hand, eq. (A.2)

has the following apparent solution,

$$p(t) = e^{\mathbb{W}t} p(0). \quad (\text{A.4})$$

While the transition matrix \mathbb{W} may not be diagonalisable, there exists an invertible matrix \mathbb{S} almost doing the job such that $\mathbb{S}^{-1}\mathbb{W}\mathbb{S} = \mathbb{J}$, where the Jordan normal form is expressed as

$$\mathbb{J} = \begin{pmatrix} \mathbb{J}_0 & 0 & \cdots & 0 \\ 0 & \mathbb{J}_1 & \cdots & 0 \\ \vdots & \vdots & \ddots & \vdots \\ 0 & 0 & \cdots & \mathbb{J}_m \end{pmatrix}, \quad (\text{A.5})$$

with the d_μ -dimensional Jordan block

$$\mathbb{J}_\mu = \begin{pmatrix} \lambda_\mu & 1 & 0 & \cdots & 0 \\ 0 & \lambda_\mu & 1 & \cdots & 0 \\ \vdots & \vdots & \ddots & \cdots & 0 \\ 0 & 0 & \cdots & \lambda_\mu & 1 \\ 0 & 0 & \cdots & 0 & \lambda_\mu \end{pmatrix}, \quad (\text{A.6})$$

and the sum over all dimensionalities of the blocks equals that of the Jordan matrix, *i.e.*,

$$\sum_{\mu} d_{\mu} = n + 1. \quad (\text{A.7})$$

Thus eq. (A.4) can be further expressed as

$$\begin{aligned} p(t) &= \mathbb{S} e^{\mathbb{S}^{-1}\mathbb{W}\mathbb{S}t} \mathbb{S}^{-1} p(0) \\ &= \mathbb{S} e^{\mathbb{J}t} \mathbb{S}^{-1} p(0) \\ &= \mathbb{S} \begin{pmatrix} e^{\mathbb{J}_0 t} & 0 & \cdots & 0 \\ 0 & e^{\mathbb{J}_1 t} & \cdots & 0 \\ \vdots & \vdots & \ddots & \vdots \\ 0 & 0 & \cdots & e^{\mathbb{J}_m t} \end{pmatrix} \mathbb{S}^{-1} p(0) \\ &= \mathbb{S} \begin{pmatrix} e^{\lambda_0 t} \cdot e^{\mathbb{Y}_0 t} & 0 & \cdots & 0 \\ 0 & e^{\lambda_1 t} \cdot e^{\mathbb{Y}_1 t} & \cdots & 0 \\ \vdots & \vdots & \ddots & \vdots \\ 0 & 0 & \cdots & e^{\lambda_m t} \cdot e^{\mathbb{Y}_m t} \end{pmatrix} \mathbb{S}^{-1} p(0), \end{aligned} \quad (\text{A.8})$$

where

$$e^{\mathbb{Y}_\mu t} = \exp[\mathbb{J}_\mu t - \text{diag}(\lambda_\mu, \lambda_\mu \cdots \lambda_\mu) t]$$

$$\begin{aligned}
&= \exp \left[\begin{pmatrix} 0 & 1 & 0 & \cdots & 0 \\ 0 & 0 & 1 & \cdots & \vdots \\ \vdots & \vdots & \ddots & \cdots & 0 \\ 0 & 0 & \cdots & 0 & 1 \\ 0 & 0 & \cdots & 0 & 0 \end{pmatrix} \cdot t \right] \\
&= \begin{pmatrix} 1 & t & \frac{t^2}{2!} & \cdots & \frac{t^{d_\mu-1}}{(d_\mu-1)!} \\ 0 & 1 & t & \cdots & \frac{t^{d_\mu-2}}{(d_\mu-2)!} \\ \vdots & \vdots & \ddots & \cdots & \vdots \\ 0 & 0 & \cdots & 1 & t \\ 0 & 0 & \cdots & 0 & 1 \end{pmatrix}. \tag{A.9}
\end{aligned}$$

That is to say, the probability distribution $p_i(t)$ can be expressed as a linear combination of the terms $\{e^{\lambda_\mu t} \cdot t^{n_\mu}\}$ ($0 \leq \mu \leq m$; $0 \leq n_\mu \leq d_\mu - 1$), which proves our conclusion that the transient states still have a stationary relative distribution in the long-time limit if their probabilities are renormalised to a finite number, and the thermalisation time scale can be described with the second largest real part of the set $\{\lambda_\mu\}$.

-
- [1] **Super-Kamiokande Collaboration**, T. Tanaka et al., *An Indirect Search for Weakly Interacting Massive Particles in the Sun Using 3109.6 Days of Upward-going Muons in Super-Kamiokande*, *Astrophys. J.* **742** (Dec., 2011) 78, [arXiv:1108.3384].
 - [2] **IceCube**, M. G. Aartsen et al., *Search for dark matter annihilations in the Sun with the 79-string IceCube detector*, *Phys. Rev. Lett.* **110** (2013), no. 13 131302, [arXiv:1212.4097].
 - [3] **ANTARES Collaboration**, S. Adrian-Martinez et al., *First results on dark matter annihilation in the Sun using the ANTARES neutrino telescope*, *JCAP* **1311** (2013) 032, [arXiv:1302.6516].
 - [4] **Baikal Collaboration**, A. Avrorin et al., *Search for neutrino emission from relic dark matter in the Sun with the Baikal NT200 detector*, arXiv:1405.3551.
 - [5] R. Bernabei et al., *Investigating electron interacting dark matter*, *Phys. Rev.* **D77** (2008) 023506, [arXiv:0712.0562].
 - [6] P. J. Fox and E. Poppitz, *Leptophilic Dark Matter*, *Phys. Rev.* **D79** (2009) 083528, [arXiv:0811.0399].
 - [7] J. Kopp, V. Niro, T. Schwetz, and J. Zupan, *DAMA/LIBRA and leptonically interacting Dark Matter*, *Phys. Rev.* **D80** (2009) 083502, [arXiv:0907.3159].

- [8] B. Feldstein, P. W. Graham, and S. Rajendran, *Luminous Dark Matter*, *Phys. Rev.* **D82** (2010) 075019, [arXiv:1008.1988].
- [9] R. Essig, J. Mardon, and T. Volansky, *Direct Detection of Sub-GeV Dark Matter*, *Phys. Rev.* **D85** (2012) 076007, [arXiv:1108.5383].
- [10] P. S. B. Dev, D. K. Ghosh, N. Okada, and I. Saha, *Neutrino Mass and Dark Matter in light of recent AMS-02 results*, *Phys. Rev.* **D89** (2014) 095001, [arXiv:1307.6204].
- [11] R. Foot, *Can dark matter - electron scattering explain the DAMA annual modulation signal?*, *Phys. Rev.* **D90** (2014), no. 12 121302, [arXiv:1407.4213].
- [12] S. K. Lee, M. Lisanti, S. Mishra-Sharma, and B. R. Safdi, *Modulation Effects in Dark Matter-Electron Scattering Experiments*, *Phys. Rev.* **D92** (2015), no. 8 083517, [arXiv:1508.07361].
- [13] B. M. Roberts, V. A. Dzuba, V. V. Flambaum, M. Pospelov, and Y. V. Stadnik, *Dark matter scattering on electrons: Accurate calculations of atomic excitations and implications for the DAMA signal*, *Phys. Rev.* **D93** (2016), no. 11 115037, [arXiv:1604.04559].
- [14] D. N. Spergel and W. H. Press, *Effect of hypothetical, weakly interacting, massive particles on energy transport in the solar interior*, *Astrophys. J.* **294** (1985) 663–673.
- [15] K. Griest and D. Seckel, *Cosmic Asymmetry, Neutrinos and the Sun*, *Nucl.Phys.* **B283** (1987) 681.
- [16] M. Nauenberg, *Energy Transport and Evaporation of Weakly Interacting Particles in the Sun*, *Phys. Rev.* **D36** (1987) 1080.
- [17] A. Gould, *WIMP Distribution in and Evaporation From the Sun*, *Astrophys. J.* **321** (1987) 560.
- [18] A. Gould and G. Raffelt, *THERMAL CONDUCTION BY MASSIVE PARTICLES*, *Astrophys. J.* **352** (1990) 654.
- [19] A. Gould, *Cosmological density of WIMPs from solar and terrestrial annihilations*, *Astrophys. J.* **388** (1992) 338–344.
- [20] S. Nussinov, L.-T. Wang, and I. Yavin, *Capture of Inelastic Dark Matter in the Sun*, *JCAP* **0908** (2009) 037, [arXiv:0905.1333].
- [21] G. Busoni, A. De Simone, and W.-C. Huang, *On the Minimum Dark Matter Mass Testable by Neutrinos from the Sun*, *JCAP* **1307** (2013) 010, [arXiv:1305.1817].
- [22] Z.-L. Liang and Y.-L. Wu, *Direct detection and solar capture of spin-dependent dark matter*, *Phys. Rev.* **D89** (2014), no. 1 013010, [arXiv:1308.5897].
- [23] R. Catena and B. Schwabe, *Form factors for dark matter capture by the Sun in effective theories*, *JCAP* **1504** (2015), no. 04 042, [arXiv:1501.03729].
- [24] A. C. Vincent, A. Serenelli, and P. Scott, *Generalised form factor dark matter in the Sun*, *JCAP* **1508** (2015), no. 08 040, [arXiv:1504.04378].
- [25] M. Blennow, S. Clementz, and J. Herrero-Garcia, *Pinning down inelastic dark matter in the Sun and in direct detection*, *JCAP* **1604** (2016), no. 04 004, [arXiv:1512.03317].
- [26] P. S. B. Dev and D. Teresi, *Asymmetric dark matter in the Sun and diphoton excess at the LHC*, *Phys. Rev.* **D94** (2016), no. 2 025001, [arXiv:1512.07243].
- [27] C. Kouvaris, *Probing Light Dark Matter via Evaporation from the Sun*, *Phys. Rev.* **D92** (2015), no. 7 075001, [arXiv:1506.04316].

- [28] A. C. Vincent, P. Scott, and A. Serenelli, *Updated constraints on velocity and momentum-dependent asymmetric dark matter*, arXiv:1605.06502.
- [29] Z.-L. Liang, Y.-L. Wu, Z.-Q. Yang, and Y.-F. Zhou, *On the evaporation of solar dark matter: spin-independent effective operators*, *JCAP* **1609** (2016), no. 09 018, [arXiv:1606.02157].
- [30] S. Baum, L. Visinelli, K. Freese, and P. Stengel, *Dark matter capture, subdominant WIMPs, and neutrino observatories*, *Phys. Rev.* **D95** (2017), no. 4 043007, [arXiv:1611.09665].
- [31] R. Garani and S. Palomares-Ruiz, *Dark matter in the Sun: scattering off electrons vs nucleons*, *JCAP* **1705** (2017), no. 05 007, [arXiv:1702.02768].
- [32] J. Smolinsky and P. Tanedo, *Dark Photons from Captured Inelastic Dark Matter Annihilation: Charged Particle Signatures*, *Phys. Rev.* **D95** (2017), no. 7 075015, [arXiv:1701.03168]. [Erratum: *Phys. Rev.* **D96**, no. 9, 099902 (2017)].
- [33] G. Busoni, A. De Simone, P. Scott, and A. C. Vincent, *Evaporation and scattering of momentum- and velocity-dependent dark matter in the Sun*, *JCAP* **1710** (2017), no. 10 037, [arXiv:1703.07784].
- [34] A. Widmark, *Thermalization time scales for WIMP capture by the Sun in effective theories*, *JCAP* **1705** (2017), no. 05 046, [arXiv:1703.06878].
- [35] M. Blennow, S. Clementz, and J. Herrero-Garcia, *The distribution of inelastic dark matter in the Sun*, *Eur. Phys. J.* **C78** (2018), no. 5 386, [arXiv:1802.06880].
- [36] A. Gould, *Resonant Enhancements in WIMP Capture by the Earth*, *Astrophys. J.* **321** (1987) 571.
- [37] A. Gould, *Direct and Indirect Capture of Wimps by the Earth*, *Astrophys. J.* **328** (1988) 919–939.
- [38] A. Serenelli, S. Basu, J. W. Ferguson, and M. Asplund, *New Solar Composition: The Problem With Solar Models Revisited*, *Astrophys. J.* **705** (2009) L123–L127, [arXiv:0909.2668].
- [39] I. F. Albuquerque, C. Perez de Los Heros, and D. S. Robertson, *Constraints on self interacting dark matter from IceCube results*, *JCAP* **1402** (2014) 047, [arXiv:1312.0797].
- [40] N. G. V. Kampen, *Stochastic processes in physics and chemistry*, North-Holland Personal Library. Elsevier, Amsterdam, third edition ed., 2007.